



Enhancement of hydration rate of LiOH by combining with mesoporous carbon for Low-temperature chemical heat storage

Mitsuhiro Kubota*, Satoshi Matsumoto, Hitoki Matsuda

Department of Chemical Systems Engineering, Graduate School of Engineering, Nagoya University, Furo-cho, Chikusa-ku, Nagoya-shi, Aichi 464-8603, Japan



HIGHLIGHTS

- Composites of LiOH and mesoporous carbon were prepared for heat storage below 373 K.
- LiOH content in the composite increased linearly with LiOH aq. concentration.
- Hydration rate was greatly enhanced by combining LiOH and mesoporous carbon.
- Both amount of water hydrated and endothermic heat increased with LiOH content.
- Most of the LiOH in the composite might react with water vapor within 10 min.

ARTICLE INFO

Keywords:

Lithium hydroxide
Mesoporous carbon
Hydration rate
Chemical heat storage

ABSTRACT

The reversible reaction between lithium hydroxide (LiOH) and lithium hydroxide monohydrate (LiOH·H₂O) is promising for low-temperature chemical heat storage below 373 K, because this system can store heat at ~340 K with a high storage density of 1440 kJ/kg. However, for practical applications, it is necessary to enhance the hydration rate of LiOH and thus achieve a higher heat release rate. In this study, we focused on a composite of LiOH and mesoporous carbon (MPC). LiOH was expected to rapidly react with the moisture condensed in the pores of MPC by capillary condensation. The LiOH/MPC composite was prepared by an impregnation method using aqueous LiOH solution concentrations of 1–10 wt% and at impregnation times of 1–48 h. It was demonstrated that LiOH was successfully supported on MPC and that the LiOH content linearly increased with increasing aqueous LiOH solution concentrations. All LiOH/MPC composites had a much higher amount of hydrated water throughout the hydration period than did LiOH or MPC, individually. Comparison of the experimental and estimated values of the amount of hydrated water and endothermic heat after 10 min of hydration showed that most of the LiOH was hydrated within 10 min in the case of the LiOH/MPC composite. From these results, it was demonstrated that LiOH supported on MPC was very effective in improving the hydration rate of LiOH.

1. Introduction

An enormous amount of low-temperature heat below 373 K is discharged from various industries into the atmosphere as waste heat. Effective utilization of such low-temperature heat is a key to establishing a society with high energy efficiency. Heat storage systems, which are classified as sensible, latent, and chemical heat storage systems, are promising technologies to bridge the time lag between heat supply and demand. Among them, chemical heat storage systems, which make use of the endothermic/exothermic nature of reversible reactions, can store heat with a high storage density without heat loss. Moreover, with such a system, it is possible to upgrade the stored heat

at an arbitrary temperature. Considering these advantages, numerous reaction systems have been proposed and studied over a wide range of storage temperatures, e.g., CaSO₄/CaSO₄·0.5H₂O [1–3], CaCl₂/CaCl₂·nH₂O [4–6], CaCl₂/CaCl₂·mNH₃ [7,8], MgO/Mg(OH)₂ [9–13], and CaO/Ca(OH)₂ [14–18] systems. Calcium sulfate hemihydrate is known to be a promising material for storing heat at ~423 K. Ogura et al. demonstrated that CaSO₄/CaSO₄·0.5H₂O system can operate in the refrigeration mode with a lab-scale experimental setup; i.e. the system can store waste heat around 393 K in the heat storing step and generate cold heat around 278 K for cooling by utilizing evaporation heat of water in the heat releasing step [3].

However, there are only a few studies on reaction systems for low-

* Corresponding author.

E-mail address: kubota.mitsuhiro@material.nagoya-u.ac.jp (M. Kubota).

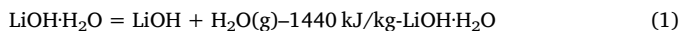
<https://doi.org/10.1016/j.applthermaleng.2019.01.049>

Received 20 February 2018; Received in revised form 14 December 2018; Accepted 17 January 2019

Available online 18 January 2019

1359-4311/ © 2019 Elsevier Ltd. All rights reserved.

temperature heat storage below 373 K. In our previous study, we measured the endothermic heat and temperature of about 30 inorganic compound hydrates using a differential scanning calorimeter [19]. The following reaction using lithium hydroxide (LiOH) was found to be the most suitable for low-temperature heat storage.



In this reaction, lithium hydroxide monohydrate ($\text{LiOH}\cdot\text{H}_2\text{O}$) can decompose into LiOH and $\text{H}_2\text{O}(\text{g})$ at 337 K with an endothermic heat of 1440 kJ/kg, meaning that $\text{LiOH}\cdot\text{H}_2\text{O}$ can store heat at ~ 340 K with a high storage density of 1440 kJ/kg in the heat storage step. Meanwhile, LiOH can release heat by reacting with $\text{H}_2\text{O}(\text{g})$ at the storage temperature or at higher temperatures in the heat releasing step. Moreover, the system is simple without side reactions, because LiOH reacts with only one mole of water vapor.

The reaction is promising for low-temperature heat storage, but it has a serious technical problem that the hydration rate of LiOH is very low. For example, the hydration ratio, which is the ratio of the amount of hydrated water to the stoichiometric one ($0.75 \text{ g}\cdot\text{H}_2\text{O}/\text{g}\cdot\text{LiOH}$), is only 0.24 even at 60 min when hydration is performed at 303 K and a relative humidity of 80%, implying that the heat output is quite low during the heat releasing step. For practical use, the hydration rate of LiOH should be greatly enhanced to achieve a higher heat output performance. To solve this problem, we have been preparing various composite materials made of LiOH and a support material. In a recent study, carbon materials such as carbon nanospheres (CNSs), multi-walled carbon nanotube (MWCNTs), activated carbon (AC), and graphene oxide (GO) were employed as nanoadditives [20–21]. The composite material was prepared by impregnating the nanoadditive into aqueous LiOH solution and characterized by scanning electron microscopy (SEM), transmission electron microscopy (TEM), X-ray diffraction (XRD), and differential scanning calorimetry (DSC). The SEM, TEM, and XRD observations indicated that nanosized crystals of $\text{LiOH}\cdot\text{H}_2\text{O}$ were dispersed on the surface of all nanoadditives except for AC. In addition, the hydration rate of all composites was greatly enhanced, and the heat storage density of the composites normalized by the $\text{LiOH}\cdot\text{H}_2\text{O}$ content was much higher than that of $\text{LiOH}\cdot\text{H}_2\text{O}$ alone. For example, the heat storage density of $\text{LiOH}\cdot\text{H}_2\text{O}/\text{CNSs}$ reached 2020 kJ/kg- $\text{LiOH}\cdot\text{H}_2\text{O}$ when hydration was conducted for 60 min at 303 K and a water vapor partial pressure of 2.97 kPa, whereas that of pure $\text{LiOH}\cdot\text{H}_2\text{O}$ was only 661 kJ/kg- $\text{LiOH}\cdot\text{H}_2\text{O}$. Similar results were obtained for the composites of $\text{LiOH}\cdot\text{H}_2\text{O}$ and other hydrophilic substances, such as polyethylene glycol (PEG), lithium chloride (LiCl), 13X-zeolite, and NaY-zeolite. Moreover, the apparent activation energy for the dehydration of the LiOH/MPC composites was greatly decreased compared to that of pure $\text{LiOH}\cdot\text{H}_2\text{O}$ due to a catalytic effect [22].

In this study, we focused on mesoporous carbon (MPC) as a support material. Mesoporous carbon is known to have a uniform mesoporous structure and can adsorb water vapor into its mesopores by capillary condensation. We expected that MPC rapidly adsorbs water vapor first and adsorbed water condensed in the mesopores might react with LiOH easily and quickly, resulting that hydration rate of LiOH would be enhanced. Moreover, MPC has good stability in alkaline solutions. The composite material of LiOH and MPC was prepared by an impregnation method at various concentrations of aqueous LiOH solutions and for impregnation times. The hydration rate of the composites was investigated using a thermogravimetric analyzer equipped with a water vapor supply system. Moreover, the heat storage density of the composites was evaluated by measuring their endothermic heat after 10 min of hydration, using DSC.

2. Experimental

2.1. Materials and preparation procedure

Lithium hydroxide monohydrate with more than 98% purity (Wako Pure Chemical Industries, Ltd.) and mesoporous carbon (Toyo Tanso Co. Ltd.) were used as starting materials. Mesoporous carbon was prepared by using magnesium oxide fine particles as a template and had a mean pore size of 3.75 nm. The BET surface area and total pore volume of the MPC were $1448 \text{ m}^2/\text{g}$ and $1.36 \text{ cm}^3/\text{g}$, respectively.

The LiOH/MPC composite was prepared by an impregnation method. First, $\text{LiOH}\cdot\text{H}_2\text{O}$ was dissolved in ion exchanged water (IEW). 0.5 g of MPC was impregnated with 20 ml of aqueous LiOH solution at a stirring rate of 600 rpm. After a predetermined impregnation time, the resulting material was recovered by filtration through filter paper No. 5C (Advantec Toyo Kaisha, Ltd.) and then dried at 423 K for 15 h in a vacuum dryer. The concentration of the aqueous LiOH solution, c , was varied from 1 to 10 wt%, and the impregnation time, θ_{im} , was 1, 24, and 48 h.

2.2. Quantitative analysis of lithium in the LiOH/MPC composite

0.5 mg of the LiOH/MPC composite, which was dried in a vacuum dryer, was soaked in 40 ml of nitric acid with a concentration of 6.9 wt %. The slurry was subjected to constant stirring at 600 rpm, at room temperature for 1 h in order to extract lithium ions from the composite material. The composite material was filtered through filter paper No. 5C (Advantec Toyo Kaisha, Ltd.). The amount of lithium in the filtrate was analyzed using inductively coupled plasma–optical emission spectroscopy (ICP-OES; Agilent Technologies, VISTA-MPX).

2.3. Characterization of LiOH/MPC composite

X-ray diffraction analysis was performed on LiOH, MPC, and the LiOH/MPC composite using an X-ray diffractometer (Rigaku Corp., RINT-TTR) with a Cu target. The pore structure (BET surface area, total pore volume, and mean pore size) of the LiOH/MPC composite was calculated by nitrogen adsorption isotherms at 77 K using a gas adsorption apparatus (Quantachrome Instruments Corp., Autosorb-1). Scanning electron micrographs were obtained with a JEOL JSM-7500FA apparatus. Transmission electron microscopy images were recorded with a JEOL EM-10000BU system.

2.4. Hydration experiments

Hydration experiments on the LiOH/MPC composites were conducted with a thermogravimetric analyzer (Shimadzu Corp., TGA-50) with a water vapor supply system. First, the composite was dehydrated at 473 K for 10 min under nitrogen atmosphere. After the temperature dropped to 303 K, the gas flow was switched to humid nitrogen at 303 K with a relative humidity of 80% at the inlet of the thermogravimetric analyzer to initiate hydration of the composite. The weight change of the composite material was recorded for 60 min. In this experiment, the hydration reaction of LiOH of the composites proceeded simultaneously with water vapor adsorption on MPC. Therefore, we define “hydration” of the LiOH/MPC composite in this paper to include both the hydration reaction and water adsorption.

The hydrated composite was sometimes removed from the thermogravimetric analyzer after a hydration time of 10 min, and its endothermic heat was measured by DSC (Shimadzu Corp., DSC-60).

3. Results and discussion

3.1. Morphological and physical properties of LiOH/MPC composite

Fig. 1 shows the XRD patterns of LiOH, MPC, and the LiOH/MPC

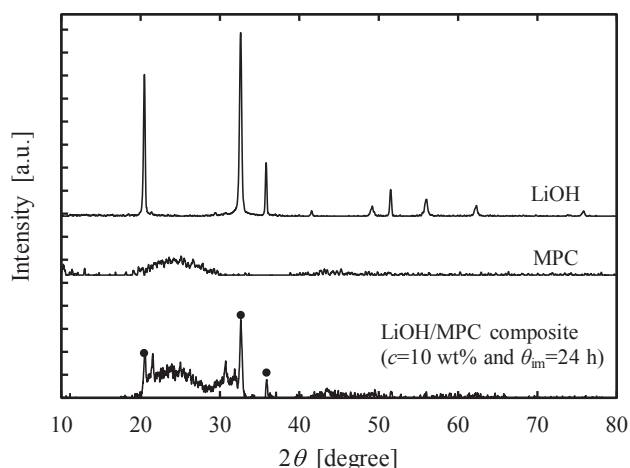


Fig. 1. XRD patterns of LiOH, MPC, and LiOH/MPC composite.

composite. The LiOH/MPC composite was prepared using 10 wt% aqueous LiOH solution at an impregnation time of 24 h. The characteristic diffraction peaks of LiOH were observed at 2θ (diffraction angle) = 20.5° , 32.6° , and 35.8° . Mesoporous carbon showed a broad weak peak between 20° and 30° . The LiOH/MPC composite exhibited not only the diffraction peak of MPC, but also the same diffraction peaks as those for LiOH.

The SEM and TEM images of MPC and the LiOH/MPC composite are shown in Figs. 2 and 3. No significant morphological differences between the samples could be seen for both figures. In addition, although crystallite size of LiOH was estimated to be about 24.7 nm according to Scherrer's equation in Fig. 1, no LiOH deposits were observed on the surface of the LiOH/MPC composite. Table 1 shows the pore structure of MPC and the LiOH/MPC composite. In every LiOH/MPC composite, the average pore size became smaller than that of the original MPC. Moreover, both the pore volume and BET surface area greatly decreased upon combining LiOH and MPC. The values of these parameters roughly decreased with increasing aqueous LiOH solution concentrations and impregnation times, and the concentration of the aqueous LiOH solution had a more noticeable effect on the pore structure than did the impregnation time. From the decrease in surface area, pore volume, and average pore size, it can be postulated that the LiOH might be supported inside of the pores of MPC.

Fig. 4 shows the effects of the preparation conditions (concentration of aqueous LiOH solution and impregnation time) on the LiOH content in the LiOH/MPC composite. The LiOH content in the composite increased linearly with an increase in the concentrations of the aqueous LiOH solution for all impregnation times. On the other hand, the LiOH content was nearly independent of the impregnation time. It is known that MPC is hydrophilic in nature and can easily disperse in water. Aqueous LiOH solution might easily reach the inner surface of MPC in a short time, so that the amount of LiOH supported was independent of impregnation time.

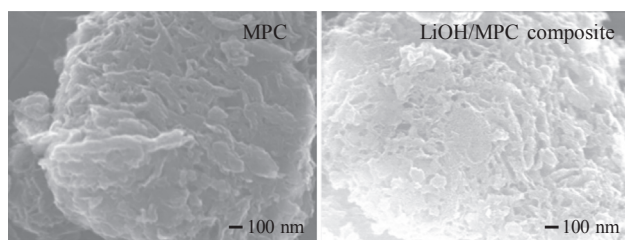


Fig. 2. SEM images of MPC and LiOH/MPC composite.

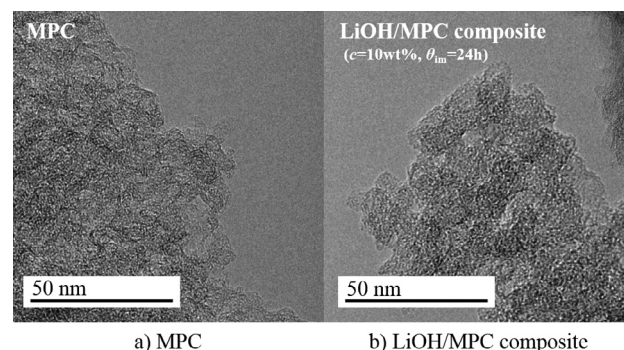


Fig. 3. TEM images of MPC and LiOH/MPC composite.

Table 1

Pore structures of MPC and the LiOH/MPC composites prepared in this study.

Sample	Aq. LiOH sola cone.	Impregnation time	Average pore size [nm]	Pore volume [cm ³ /g]	Specific surface area [m ² /g]
MPC			3.75	1.36	1448
LiOH/MPC	1 wt%	1 h	3.48	1.14	1311
	1 wt%	24 h	3.43	0.98	1140
	1 wt%	48 h	3.40	0.96	1125
	5 wt%	1 h	3.42	0.77	898
	5 wt%	24 h	3.41	0.64	756
	5 wt%	48 h	3.40	0.72	846
	10 wt%	1 h	3.43	0.57	660
	10 wt%	24 h	3.42	0.53	622
	10 wt%	48 h	3.39	0.58	687

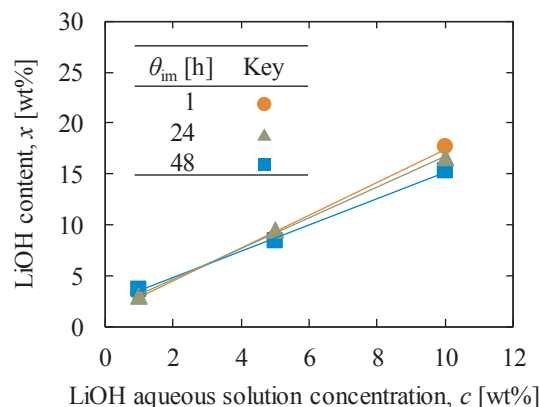


Fig. 4. Effects of various aqueous LiOH solution concentrations and impregnation times on LiOH content in the LiOH/MPC composite.

3.2. Hydration behaviors of the LiOH/MPC composite

Fig. 5 shows the temporal change in the amount of hydrated water for LiOH, MPC, and the LiOH/MPC composite prepared at $c = 5$ wt% and $\theta_{im} = 24$ h when each sample was hydrated at 303 K with a relative humidity of 80%. Lithium hydroxide gradually reacted with water vapor, and the amount of hydrated water monotonically increased with time. The amount of hydrated water of LiOH was 0.18 g-H₂O/g-sample at 60 min, but the hydration ratio was only 0.24. Mesoporous carbon adsorbed water vapor quickly and almost reached the equilibrium state within 20 min. The equilibrium amount of water vapor was 0.21 g-H₂O/g-sample at 60 min. Meanwhile, the hydration of the LiOH/MPC composite proceeded rapidly with a higher hydration rate than that for LiOH and MPC; for example, the average hydration rate of the LiOH/MPC composite was 2.23×10^{-2} g-H₂O/(g-sample min) for the initial period of 10 min, whereas those of LiOH and MPC were 0.50×10^{-2}

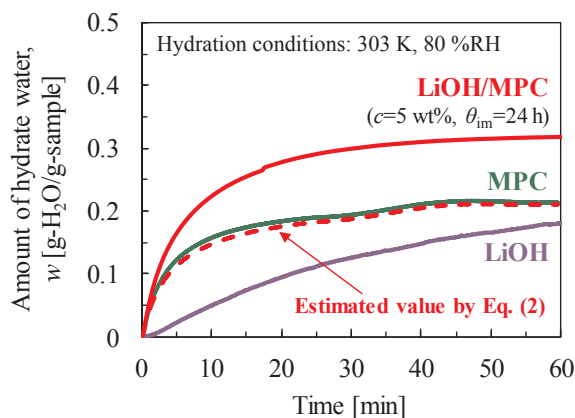


Fig. 5. Temporal changes in amount of hydrate water for LiOH, MPC, and LiOH/MPC composite when hydration was performed at 303 K and 80 %RH.

and 1.57×10^{-2} g-H₂O/(g-sample min), respectively. Further, the LiOH/MPC composite had a greater amount of hydrated water (0.32 g-H₂O/g-sample) than did LiOH or MPC (0.18 or 0.21 g-H₂O/g-sample, respectively) after hydration for 60 min.

If LiOH and MPC react with water vapor independent of each other, the amount of hydrated water of the LiOH/MPC composite could be estimated from the following equation.

$$w_{\text{est}} = w_{\text{LiOH}} \times \left(\frac{x}{100}\right) + w_{\text{MPC}} \times \left(1 - \frac{x}{100}\right) \quad (2)$$

where w_{LiOH} and w_{MPC} represent the amounts of hydrated water for LiOH and MPC, respectively, at a given time when only LiOH or MPC is hydrated at 303 K with a relative humidity (RH) of 80%, and x is the LiOH content. The estimated hydration curve is also shown in Fig. 5. The estimated data for the LiOH/MPC composite indicated a similar shape as that for the MPC, because the composite material contained only 9.4 wt% of LiOH, as expected from the low hydration rate of LiOH. A significant difference was observed when comparing the experimental and estimated values for the LiOH/MPC composite, and the experimental values were much higher. From these results, it is revealed that the combination of LiOH and MPC is very effective at promoting the hydration reactivity of LiOH.

3.3. Effect of preparation conditions on hydration behaviors of the LiOH/MPC composite

Fig. 6 shows the hydration curve of the LiOH/MPC composites prepared with various concentrations of aqueous LiOH solution and at impregnation times of 1–48 h. All LiOH/MPC composites indicated a larger amount of hydrated water as compared to those of LiOH or MPC at a given time. The amount of hydrated water in the composites

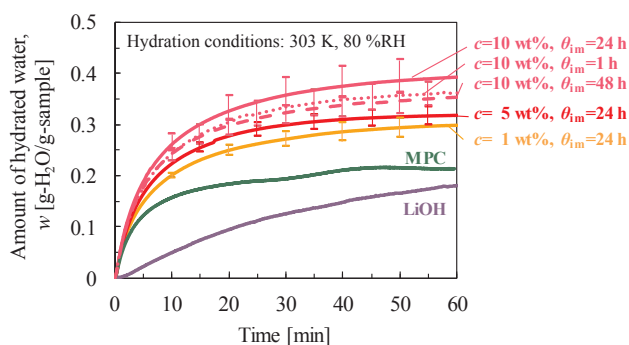


Fig. 6. Hydration curves of LiOH/MPC composite prepared at various LiOH aqueous solution concentrations and impregnation times.

increased with increasing concentrations of aqueous LiOH solution, and the value at $c = 10$ wt% and $\theta_{\text{im}} = 24$ h reached a maximum of 0.39 g-H₂O/g-sample in 60 min. Meanwhile, the impregnation time did not greatly affect the hydration behavior of the composite. As shown in Fig. 4, the LiOH content in the composite increased with increasing concentrations of the aqueous LiOH solution, but was almost independent of impregnation time. From these results, the improvement of the hydration rate could be attributed to the increased LiOH content in the composite. In our previous studies, we have prepared some LiOH-based composites by combining with hydrophilic substances or carbon nanoadditives. The LiOH/hydrophilic substance composites achieved the best amount of hydrated water of 0.52–0.54 g-H₂O/g-sample when hydration was conducted for 60 min at 303 K with a relative humidity of around 70% [22]. The LiOH/carbon nanoadditive composites also had that of 0.27–0.31 g-H₂O/g-sample [20]. On the other hand, LiOH/MPC composite in this study showed the amount of hydrated water of 0.39 g-H₂O/g-sample at 303 K and RH = 80%. From these results, it is found that LiOH/MPC composites had hydration performance at least equal to or higher than the LiOH/carbon nanoadditive composites.

We conducted a fundamental study on cycle stability of the composite by repeating dehydration and hydration reactions for 20 cycles. Dehydration was performed at 393 K for 30 min, whereas hydration was conducted at 303 K for 100 min. Throughout the experiment, humid air at an absolute humidity of 21.6 g-H₂O/kg-Dry air, whose relative humidity was 80% at 303 K, was supplied to the inlet of the thermogravimetric analyzer. As a result, the amount of hydrated water of the composite fluctuated randomly during cycle reactions. Although hydrated water after 2 cycles decreased by an average of 11% compared to that in 1st cycle, it was almost kept within 20 cycles. Consequently, LiOH/MPC composite might have high cycle stability. However, a further research on cycle stability is required towards a practical use of the composite.

Fig. 7 shows the relationship between the LiOH content in the composite and the amount of hydrated water at 10 min. Similarly, the relationship between LiOH content and endothermic heat of the composite after 10 min of hydration, which corresponds to heat storage capacity for 10 min, is shown in Fig. 8. In Fig. 8, two endothermic heats of MPCs are plotted at the LiOH content of 0 wt%. One is for the raw MPC, and another is for the MPC soaked into ion exchanged water (IEW) for 24 h, that is the same impregnation time for preparing LiOH/MPC composites. It can be seen that endothermic heat of MPC increased from 324.5 kJ/kg to 409.9 kJ/kg by the treatment with IEW. A similar trend that MPC treated with IEW had a higher amount of hydrated water than the raw one is also observed in Fig. 7. Shimooka et al. reported that the amount of adsorbed water on porous carbon increased with the amount of surface oxygen functional groups [23]. Reinoso et al. also reported that the amount of surface oxygen functional groups increased upon impregnating porous carbon with an alkali solution [24]. Consequently, an increase in the endothermic heat of MPC itself

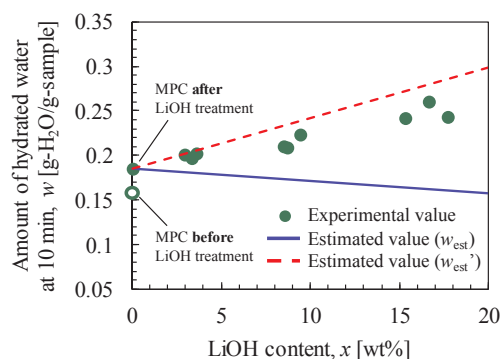


Fig. 7. Effects of LiOH content on the amount of hydrated water after 10 min of hydration at 80 %RH.

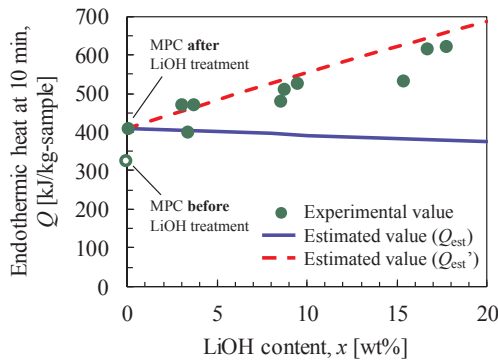


Fig. 8. Effects of LiOH content on endothermic heat after 10 min of hydration at 80 %RH.

might be attributed to the increased amount of adsorbed water accompanied by the increasing amount of surface oxygen functional groups. In Figs. 7 and 8, it is also found that both the amount of water hydrated and the endothermic heat of the hydrated LiOH/MPC composite at 10 min increased linearly with an increase in the LiOH content. In Fig. 7, the line represents a change in the amount of hydrated water of the LiOH/MPC composite. A value similar to that in Fig. 7, calculated by Eq. (3) under the same assumption made in Eq. (2), is plotted in Fig. 8.

$$Q_{est} = \frac{(1 + w_{LiOH}) \times \left(\frac{x}{100}\right) \times \Delta H_{LiOH \cdot H_2O} + (1 + w_{MPC}) \times \left(1 - \frac{x}{100}\right) \times \Delta H_{MPC}}{(1 + w_{LiOH}) \times \left(\frac{x}{100}\right) + (1 + w_{MPC}) \times \left(1 - \frac{x}{100}\right)} \quad (3)$$

where w_{LiOH} and w_{MPC} are the amounts of hydrated water for LiOH and MPC, respectively, after 10 min of hydration, $\Delta H_{LiOH \cdot H_2O}$ is endothermic heat of $LiOH \cdot H_2O$ ($\Delta H_{LiOH \cdot H_2O} = 1440$ kJ/kg), and ΔH_{MPC} is endothermic heat of MPC after 10 min of hydration ($\Delta H_{MPC} = 409.9$ kJ/kg). In both figures, the values calculated using Eqs. (2) and (3) decreased with an increase in the LiOH content and showed an opposite trend as compared to the experimental values. Moreover, the experimental values in Figs. 7 and 8 were much larger than the estimated values within the experimental range of LiOH content, indicating that the hydration of LiOH was promoted by using MPC as a support. Assuming that LiOH reacts completely with water vapor within 10 min of hydration, the amount of hydrated water and endothermic heat of the LiOH/MPC composite were estimated from the following equations.

$$w_{est} = w_{LiOH \cdot H_2O} \times \left(\frac{x}{100}\right) + w_{MPC} \times \left(1 - \frac{x}{100}\right) \quad (4)$$

$$Q_{est} = \frac{w_{LiOH \cdot H_2O} \times \left(\frac{x}{100}\right) \times \left(\frac{MW_{LiOH \cdot H_2O}}{MW_{H_2O}}\right) \times \Delta H_{LiOH \cdot H_2O} + (1 + w_{MPC}) \times \left(1 - \frac{x}{100}\right) \times \Delta H_{MPC}}{(1 + w_{LiOH \cdot H_2O}) \times \left(\frac{x}{100}\right) + (1 + w_{MPC}) \times \left(1 - \frac{x}{100}\right)} \quad (5)$$

where $w_{LiOH \cdot H_2O}$ is the amount of hydrated water when LiOH completely reacted with water vapor, $w_{LiOH \cdot H_2O} = MW_{H_2O}/MW_{LiOH}$, w_{MPC} is the amount of hydrated water after 10 min of hydration of MPC, $\Delta H_{LiOH \cdot H_2O}$ is the endothermic heat of $LiOH \cdot H_2O$ ($\Delta H_{LiOH \cdot H_2O} = 1440$ kJ/kg), and ΔH_{MPC} is endothermic heat of MPC after 10 min of hydration ($\Delta H_{MPC} = 409.9$ kJ/kg). The estimated values based on Eqs. (4) and (5) are also plotted as broken lines in Figs. 7 and 8, respectively. In both figures, it can be seen that the estimated values are higher than the experimental values but follow the same trend. From these results, it is suggested that the hydration of LiOH was greatly enhanced by supporting it on MPC and that most of the hydration might be completed in 10 min. However, further research is

required to reveal the reason underlying the hydration enhancement of the LiOH/MPC composite.

4. Conclusion

For the establishment of a society with high energy utilization efficiency, we focused on a chemical heat storage technology that can not only store heat energy with high storage density but also release the stored heat at a desired temperature. Among the various reactions studied, the $LiOH/LiOH \cdot H_2O$ reaction was promising for low-temperature heat storage below 373 K, because it could store heat at ~ 340 K with storage density of 1440 kJ/kg. However, a key issue with implementing this in a practical way is that the hydration rate of LiOH is very low, meaning that heat output performance is too low. In this study, a combination of LiOH and MPC with uniform mesopores was tested for promoting the reactivity of LiOH with water vapor. LiOH/MPC composites were prepared by an impregnation method at various LiOH aqueous solution concentrations of $c = 1$ –10 wt% and impregnation times of $\theta_{im} = 1$ –48 h. From the change in pore structure of the composite, it was surmised that LiOH was supported inside the pore of MPC, demonstrating that the LiOH/MPC composite was successfully prepared. The LiOH content in the LiOH/MPC composite linearly increased with an increase in the concentration of the aqueous LiOH solution but was independent of the impregnation time. From the hydration experiments, all LiOH/MPC composites achieved much higher initial hydration rates and the amount of hydrated water at 60 min than did LiOH or MPC individually. The amount of hydrated water and endothermic heat of LiOH/MPC composite increased with increasing LiOH content. The LiOH/MPC composite prepared at $c = 10$ wt% and $\theta_{im} = 24$ h showed 5.3 and 1.7 times higher hydration rate at 10 min than did LiOH and MPC, respectively. Comparison of the experimental amount of hydrated water at 10 min with the estimated values suggested that most of the LiOH in the composite reacted with water vapor in 10 min.

Acknowledgement

This research was partially supported by The Thermal & Electric Energy Technology Foundation.

Appendix A. Supplementary material

Supplementary data to this article can be found online at <https://doi.org/10.1016/j.applthermaleng.2019.01.049>.

References

- [1] J.H. Lee, H. Ogura, S. Sato, Reaction control of $CaSO_4$ during hydration/dehydration repetition for chemical heat pump system, *Appl. Therm. Eng.* 63 (2014) 192–199.
- [2] H. Ogura, H. Mikami, H. Suzuki, Enhancement of refrigeration cold-heat production by thermal driven chemical heat pump, *Trans. Jpn. Soc. Refrig. Air Cond. Eng.* 32 (3) (2015) 373–379.
- [3] H. Ogura, M. Kubota, H. Suzuki, T. Yamakawa, Fundamental experimental study on chemical heat pump for storing low-temperature waste heat and releasing cold-heat, *Kagaku Kogaku Ronbunshu* 35 (5) (2009) 506–510.
- [4] T. Esaki, M. Yasuda, N. Kobayashi, Experimental evaluation of the heat output/input and coefficient of performance characteristics of a chemical heat pump in the heat upgrading cycle of $CaCl_2$ hydration, *Energy Convers. Manage.* 150 (2017) 365–374.
- [5] K.E. NTsoukpo, H.U. Rammelberg, A.F. Lele, K. Korhammer, B.A. Watts, T. Schmidt, W.K.L. Ruck, A review on the use of calcium chloride in applied thermal engineering, *Appl. Therm. Eng.* 75 (2015) 513–531.
- [6] M. Molenda, J. Stengler, M. Linder, A. Wörner, Reversible hydration behavior of $CaCl_2$ at high H_2O partial pressures for thermochemical energy storage, *Thermochim. Acta* 560 (2013) 76–81.
- [7] M. van der Pal, R.E. Critoph, Performance of $CaCl_2$ -reactor for application in ammonia-salt based thermal transformers, *Appl. Therm. Eng.* 126 (2017) 518–524.
- [8] L. Jiang, A.P. Roskilly, R.Z. Wang, L.W. Wang, Y.J. Lu, Analysis on innovative modular sorption and resorption thermal cell for cold and heat cogeneration, *Appl. Energy* 204 (2017) 767–779.

- [9] E. Mastronardo, L. Bonaccorsi, Y. Kato, E. Piperopoulos, M. Lanza, C. Milone, Strategies for the enhancement of heat storage materials performances for $\text{MgO}/\text{H}_2\text{O}/\text{Mg}(\text{OH})_2$ thermochemical storage system, *Appl. Therm. Eng.* 120 (2017) 626–634.
- [10] S. Li, H. Huang, X. Yang, C. Wang, N. Kobayashi, M. Kubota, A facile method to construct graphene oxide-based magnesium hydroxide for chemical heat storage, *Nanoscale Microscale Thermophys. Eng.* 21 (1) (2017) 1–7.
- [11] A. Shkatulov, Y. Aristov, Modification of magnesium and calcium hydroxides with salts: An efficient way to advanced materials for storage of middle-temperature heat, *Energy* 85 (2015) 667–676.
- [12] J. Ryu, T. Mizuno, H. Ishitobi, Y. Kato, Dehydration and hydration behavior of Mg-Co mixed hydroxide as a material for chemical heat storage, *J. Chem. Eng. Jpn.* 47 (7) (2014) 579–586.
- [13] A. Shkatulov, T. Krieger, V. Zaikovskii, Y. Chesalov, Y. Aristov, Doping magnesium hydroxide with sodium nitrate: a new approach to tune the dehydration reactivity of heat-storage materials, *ACS Appl. Mater. Interf.* 22 (2014) 19966–19977.
- [14] H. Zhang, H. Ogura, M. Umez, T. Imai, M. Ishii, Hydration reaction characteristics of CaO from various local limestone samples as chemical heat pump/storage materials, *J. Mater. Sci.* 52 (2017) 11360–11369.
- [15] J. Kariya, J. Ryu, Y. Kato, Development of thermal storage material using vermiculite and calcium hydroxide, *Appl. Therm. Eng.* 94 (2016) 186–192.
- [16] Y.A. Criado, M. Alonso, J.C. Abanades, Z. Anxionnaz-Minvielle, Conceptual process design of a $\text{CaO}/\text{Ca}(\text{OH})_2$ thermochemical energy storage system using fluidized bed reactors, *Appl. Therm. Eng.* 73 (2014) 1087–1094.
- [17] F. Watanabe, S. Tsumagari, H. Huang, M. Hasatani, N. Kobayashi, O. Tsubouchi, N. Shiomi, Performance evaluation of carbonaceous porous solid supported $\text{Ca}(\text{OH})_2$ chemical heat storage material, *Kagaku Kogaku Ronbunshu* 39 (4) (2013) 378–383.
- [18] F. Schaube, L. Koch, A. Worner, Müller-Steinhagen, A thermodynamic and kinetic study of the de- and rehydration of $\text{Ca}(\text{OH})_2$ at high H_2O partial pressures for thermo-chemical heat storage, *Thermochim. Acta* 538 (2012) 9–20.
- [19] M. Kubota, S. Matsumoto, H. Matsuda, H. Huang, Z. He, X. Yang, Chemical heat storage with $\text{LiOH}/\text{LiOH}\cdot\text{H}_2\text{O}$ reaction for low-temperature heat below 373 K, *Adv. Mater. Res.* 953–954 (2014) 757–760.
- [20] X. Yang, S. Li, H. Huang, J. Li, N. Kobayashi, M. Kubota, Effect of carbon nanoadditives on lithium hydroxide monohydrate-based composite materials for low temperature chemical heat storage, *Energies* 10 (5) (2017) 644.
- [21] X. Yang, H. Huang, Z. Wang, M. Kubota, Z. He, N. Kobayashi, Facile synthesis of graphene oxide-modified lithium hydroxide for low-temperature chemical heat storage, *Chem. Phys. Lett.* 644 (2016) 31–34.
- [22] S. Li, H. Huang, X. Yang, Y. Bai, J. Li, N. Kobayashi, M. Kubota, Hydrophilic substance assisted low temperature $\text{LiOH}\cdot\text{H}_2\text{O}$ based composite thermochemical materials for thermal energy storage, *Appl. Therm. Eng.* 128 (2017) 706–711.
- [23] S. Shimooka, M. Yamazaki, T. Takewki, E. Akashige, F. Ikehata, H. Kakiuchi, F. Watanabe, M. Kubota, H. Matsuda, Development of hydrophilic active carbon for high performance adsorption heat pump, *Kagaku Kogaku Ronbunshu* 32 (6) (2006) 528–534.
- [24] F.R. Reinoso, M.M. Sabio, M.A. Muñecas, Effect of microporosity and oxygen surface groups of activated carbon in the adsorption of molecules of different polarity, *Electrochim. Acta* 56 (2010) 657–662.